Shifting carbon flow from roots into associated microbial communities in response to elevated atmospheric CO_2

Barbara Drigo[a,b], Agata S. Pijl[a], Henk Duyts[c], Anna M. Kielak[a], Hannes A. Gamper[a], Marco J. Houtekamer[d], Henricus T. S. Boschker[d], Paul L. E. Bodelier[e], Andrew S. Whiteley[f], Johannes A. van Veen[a,g], and George A. Kowalchuk[a,h,1]

[a]Department of Microbial Ecology, The Netherlands Institute of Ecology (NIOO-KNAW), 6666 ZG, Heteren, The Netherlands; [b]Centre for Plants and the Environment, University of Western Sydney, Penrith South DC, New South Wales 1797, Australia; [c]Department of Terrestrial Ecology, The Netherlands Institute of Ecology (NIOO-KNAW), 6666 ZG, Heteren, The Netherlands; [d]Department of Marine Microbiology, The Netherlands Institute of Ecology (NIOO-KNAW), 4400 AC, Yerseke, The Netherlands; [e]Department of Microbial Ecology, The Netherlands Institute of Ecology (NIOO-KNAW), 3600 BG, Nieuwersluis, The Netherlands; [f]Biodiversity and Ecosystem Function Group, Molecular Microbial Ecology Section, Centre for Ecology and Hydrology, Oxford OX1 3SR, United Kingdom; [g]Institute of Biology, Leiden University, 2300 RA, Leiden, The Netherlands; and [h]Institute of Ecological Science, Vrije Universiteit, 1081 HV, Amsterdam, The Netherlands

Rising atmospheric CO_2 levels are predicted to have major consequences on carbon cycling and the functioning of terrestrial ecosystems. Increased photosynthetic activity is expected, especially for C-3 plants, thereby influencing vegetation dynamics; however, little is known about the path of fixed carbon into soil-borne communities and resulting feedbacks on ecosystem function. Here, we examine how arbuscular mycorrhizal fungi (AMF) act as a major conduit in the transfer of carbon between plants and soil and how elevated atmospheric CO_2 modulates the belowground translocation pathway of plant-fixed carbon. Shifts in active AMF species under elevated atmospheric CO_2 conditions are coupled to changes within active rhizosphere bacterial and fungal communities. Thus, as opposed to simply increasing the activity of soil-borne microbes through enhanced rhizodeposition, elevated atmospheric CO_2 clearly evokes the emergence of distinct opportunistic plant-associated microbial communities. Analyses involving RNA-based stable isotope probing, neutral/phosphate lipid fatty acids stable isotope probing, community fingerprinting, and real-time PCR allowed us to trace plant-fixed carbon to the affected soil-borne microorganisms. Based on our data, we present a conceptual model in which plant-assimilated carbon is rapidly transferred to AMF, followed by a slower release from AMF to the bacterial and fungal populations well-adapted to the prevailing (myco-)rhizosphere conditions. This model provides a general framework for reappraising carbon-flow paths in soils, facilitating predictions of future interactions between rising atmospheric CO_2 concentrations and terrestrial ecosystems.

^{13}C | arbuscular mycorrhizal | climate change | RNA-based stable isotope probing | rhizosphere

Anthropogenic CO_2 emissions are clearly contributing to rising atmospheric CO_2 levels, but the future rate of atmospheric CO_2 elevation remains uncertain (1). A major contribution to this uncertainty is our lack of knowledge concerning the path of carbon flow through plants into the soil and the potential for climate–carbon cycle feedbacks involving vegetated terrestrial ecosystems (1). Elevated atmospheric CO_2 leads to higher C assimilation by plants (2), and root-soil interactions facilitate movement of C to the soil (3), which represents the largest and most stable C pool in the terrestrial biosphere (4). In addition to potential long-term changes in litter quantity and quality, C fixed by plants can enter the soil through increased root turnover, greater sloughing off of cells, enhanced plant tissue breakdown, or increased root exudation (3–6). Plant-derived exudates provide energy for rhizosphere microbial communities, thereby influencing their structure and function (2–8). Arbuscular mycorrhizal fungi (AMF) form symbioses with the majority of land plants (9, 10) and have been recognized as a potentially important functional group involved in the

sequestration of plant-derived C (9–11). Although recent progress has been made in our understanding of C fluxes from the plant to AMF, rhizosphere microorganisms, and the soil–food web, knowledge is still scarce with respect to the relative flow of C to specific biological groups in plant–soil systems (3–12). Such knowledge is critical to our understanding of carbon cycling in terrestrial ecosystems and to assessing soil carbon-storage potential in mitigating rising atmospheric CO_2 conditions.

The application of ^{13}C stable isotope probing (SIP) (13–15) to track plant-derived C fluxes into microbial nucleic acids (13, 14) or other biomarkers (15) has opened up a window to understanding the flux of C through plant-associated microbial communities. To track the fate of plant-assimilated C to belowground microbial communities in response to elevated atmospheric CO_2, we conducted a $^{13}CO_2$ pulse-chase labeling experiment with *Festuca rubra* (mycorrhizal C-3 grass species) and *Carex arenaria* (non-mycorrhizal C-3 sedge) plants grown for 6 months under ambient (350 ppm) or elevated (700 ppm) CO_2 conditions. Using RNA and neutral/phosphate lipid fatty acids (N/PLFA) SIP, community fingerprinting, and taxon-specific real-time PCR, we tracked active microbial populations in situ, focusing on total bacterial, total fungal, *Pseudomonas* spp., *Burkholderia* spp., *Bacillus*, actinomycetes, and protozoan communities. This allowed us to track, both specifically and temporally, the distribution of plant-assimilated carbon through soil-borne communities and to compare the responses of the different microbial groups to the C pathways under ambient versus elevated CO_2 for the two contrasting plant species studied.

Results and Discussion

For *F. rubra*, AMF signature biomarkers (N/PLFA 16:1ω5) (12) showed strong ^{13}C labeling within 1 day, followed by a significant decrease ($P < 0.001$), reaching a baseline 14 days after labeling (Fig. 1). NLFA 16:1ω5 enrichment was significantly increased at elevated CO_2 from days 1 to 5 (Fig. 1A) (days × CO_2: $F_{7,14} = 920.14$; $P < 0.001$), and PLFA 16:1ω5 enrichment at elevated CO_2
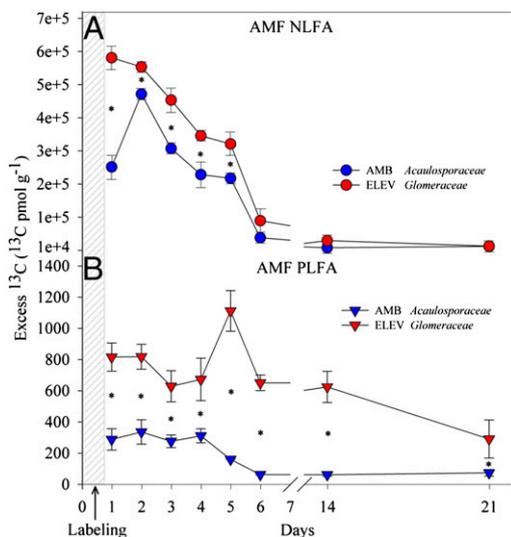
Fig. 1. ^{13}C enrichment in the AMF signatures 16:1ω5 determined in *F. rubra* rhizosphere soil for NFLA (circles; *A*) and PLFA (triangles; *B*) at ambient CO_2 (blue) and elevated CO_2 (red). The given AMF families, *Acaulosporaceae* and *Glomeraceae*, denote the affiliations of the 18S rRNA gene fragments recovered from the ^{13}C-labeled RNA fractions by RNA-SIP at ambient CO_2 and elevated CO_2, respectively. Asterisks designate significant differences ($P < 0.001$) between CO_2 concentrations. The values given are the average of biological replicates, and errors represent the standard error.

was significantly higher during the entire incubation period (Fig. 1*B*) (days × CO_2: $F_{7,4} = 1,682.53$; $P < 0.001$). Increased ^{13}C labeling of NLFA suggested enhanced production of AMF storage organs, and increased ^{13}C labeling of PLFA implied AMF growth stimulation (12). These data confirm earlier results (12–16) on the dominant role of AMF in the flow of C from plants into the

soil and show that a large proportion of photoassimilated ^{13}C flows from the plant to the AMF, with only a minor fraction directly transferred to the bacterial community in the rhizosphere. We also observed a temporally synchronized pattern in the labeling of the rhizosphere fractions, with the major labeling of the rhizosphere bacteria coinciding with the gradual decrease of the ^{13}C content of the AMF, suggesting that the majority of the ^{13}C that is assimilated by the bacterial rhizosphere community is derived from AMF turnover.

RNA-SIP revealed a complete shift in the dominant AMF species receiving plant-derived C under ambient versus elevated CO_2 conditions (Fig. 1 and Fig. S1 *B1* and *B2*). Based on PCR-denaturing gradient gel electrophoresis (DGGE) and cloning analyses, it was apparent that, at ambient atmospheric CO_2 conditions, virtually all of the C entering the AMF community was channeled to a single AMF taxon affiliated to the Acaulosporaceae (*A. lacunose*-like), whereas, under elevated CO_2, the dominant AMF incorporating ^{13}C label was a population affiliated to the Glomeraceae (*G. claroideum*-like). These two AMF families are known to exploit different niches and exhibit disparate life-history strategies (17). Fungal-specific 18S rRNA gene clone libraries were also in accordance with a greater C allocation to AMF at elevated CO_2, with ^{13}C-labeled fractions taken 1 day after pulse labeling yielding ~84% AMF sequences at elevated CO_2 compared with 60% AMF sequences at ambient atmospheric CO_2 concentrations ($P < 0.001$) (Fig. S2).

Elevated CO_2 conditions also significantly affected the spectrum of non-AMF fungi incorporating plant-derived C ($P > 0.001$), mirroring previously observed changes in fungal community structure in response to elevated CO_2 (18). Differences included the presence of *Trichoderma harzianum* (Hypocreaceae), *Eimeriidae*-like sequences, and an unidentified fungal species at ambient CO_2 6 days after labeling and the absence of *Trichosporon porosum* (Basidiomycota), *Capnobotrytella* sp., and *Heteroconium chaetospira*-like (Herpotrichiellaceae) sequences from the ^{13}C-labeled fractions associated with plants grown at elevated CO_2 (Fig. S2).
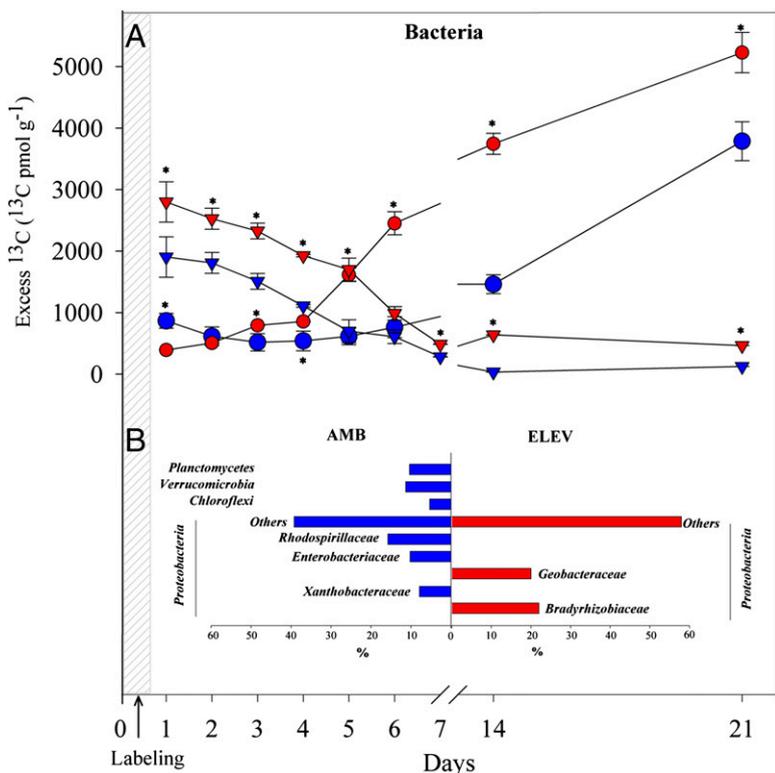
Fig. 2. (*A*) ^{13}C enrichment in the bacterial PLFAs at ambient CO_2 (blue) and elevated CO_2 (red) in the rhizosphere soil of *F. rubra* (circles) and *C. arenaria* (triangles). Asterisks ($P < 0.001$) designate significant differences between CO_2 concentrations. The values given are the average of the different biological replicates, and errors represent the standard error. (*B*) Significantly different groups in clone libraries derived from *F. rubra* ^{13}C-labeled 16S rRNA at ambient (blue) and elevated (red) CO_2, harvested 21 days after labeling.

The gradual decrease of the ^{13}C incorporation in AMF-specific biomarkers was accompanied by a significant increase ($P < 0.001$) in ^{13}C incorporation by the bacterial community, commencing 4–5 days after labeling in the mycorrhizal plant (*F. rubra*) (Fig. 2*A*). The nonmycorrhizal plant, *C. arenaria*, showed a contrasting pattern, with a rapid incorporation of ^{13}C by the bacterial community at the outset of the experiment that was directly followed by a decrease (Fig. 2*A*). PCR-cloning analyses based on ^{13}C-labeled 16S rRNA fractions showed a significant effect of CO_2 treatment ($P < 0.001$), in agreement with observed shifts in total bacterial community structure (18). Shifts in dominant C-incorporating bacteria were observed during the course of the experiment (Fig. 2*B*). For instance, at ambient CO_2 for *F. rubra*, Proteobacteria represented 68%, 84%, 93%, 96%, and 73% of bacterial sequences 1, 3, 6, 14, and 21 days postlabeling, respectively (Fig. S2). The remaining sequences were mostly affiliated with Chloroflexi, Planctomycetes, and Verrucomicrobia, with the last only detected in the ^{13}C fraction at day 21 (Fig. 2*B* and Fig. S2). At elevated CO_2, all clones derived from ^{13}C fractions were affiliated with Proteobacteria (Fig. 2*B* and Fig. S2). Within the Proteobacteria, significant differences ($P < 0.001$) were observed between the ^{13}C-labeled bacterial clone libraries derived from the ambient versus elevated CO_2 treatments at all sampling times. Differences included the presence of the Xanthobacteraceae-, Rhodospirillaceae-, and Enterobacteriaceae-like sequences only in ambient CO_2 libraries and Geobacteraceae- and Bradyrhizobiaceae-like sequences only in the elevated CO_2 libraries. Interestingly, within this last family, *Bradyrhizobium japonicum*-like sequences were detected. This species has been identified as mycorrhizal helper bacteria (MHB) of the AMF genus *Glomus* (10).

For both plant species, the peak of ^{13}C incorporation into protozoan biomass, as judged by PLFA 20:4ω6 (19) (Fig. S3*A*), coincided with the highest ^{13}C incorporation into the bacterial community, 5–6 days and 1 day postlabeling for *F. rubra* and *C. arenaria*, respectively (Fig. 2*A*), suggesting a coupling of bacterial and protozoan growth.

Typical rhizosphere bacterial groups (20) also showed a pronounced response to the CO_2 treatment throughout the labeling experiment. At ambient CO_2, *Pseudomonas fluorescens* was the main *Pseudomonas* species incorporating plant-derived C (Fig. 3). This species is also known to function as an MHB, enhancing AMF development (10). Under elevated CO_2, the diversity of the active *Pseudomonas* community increased, with active populations of *P. fluorescens*, *P. aeruginosa*, *P. trivialis*, and *P. putida* being detected (Fig. 3*A*). Isolates of several of these species have been shown to have MHB, biocontrol, or pathogenic activities (10). Large shifts were also observed within dominant C-incorporating Burkholderiaceae species, with an opposite trend with respect to diversity. Populations affiliated with *B. fungorum*, *B. cepacia*, *B. glathei*, *B. phenazinum*, *B. xenoforans*, and an unidentified *Burkholderia* species (unknown 2, 4 degrading bacteria) were detected at elevated CO_2, yet only the last three of these species were detected at ambient CO_2 (Fig. 3*B*). To quantify C uptake by *Pseudomonas* ssp. and *Burkholderia* ssp., the cyclopropyl PLFAs cy17:0 and cy19:0 were used as biomarkers for *Pseudomonas* spp. and *Burkholderia* spp., respectively (21). As judged by these biomarkers, these genera became highly enriched in ^{13}C for *F. rubra* at elevated CO_2 (Fig. 3). This coincided with a lower biomass (Fig. S1 *A1* and *A2*), suggesting a more rapid turnover at elevated CO_2.

At ambient atmospheric conditions, mycorrhizal fungi have been estimated to receive up to 20% of the plant photosynthetates (22). In our study, the total incorporation of plant photosynthetates into mycorrhizal fungi was up to 30% of the total fixed ^{13}C in *F. rubra* rhizosphere soil at ambient atmospheric CO_2 and up to 40% at elevated CO_2 (Fig. S4). Trehalose synthesis is thought to contribute to C drain through mycorrhizal fungi (10) and to play an important role in selecting specific bacterial communities in the mycorrhizosphere, specifically members of the genera *Bradyrhizobia*, *Pseudomonas*, and *Bur-*
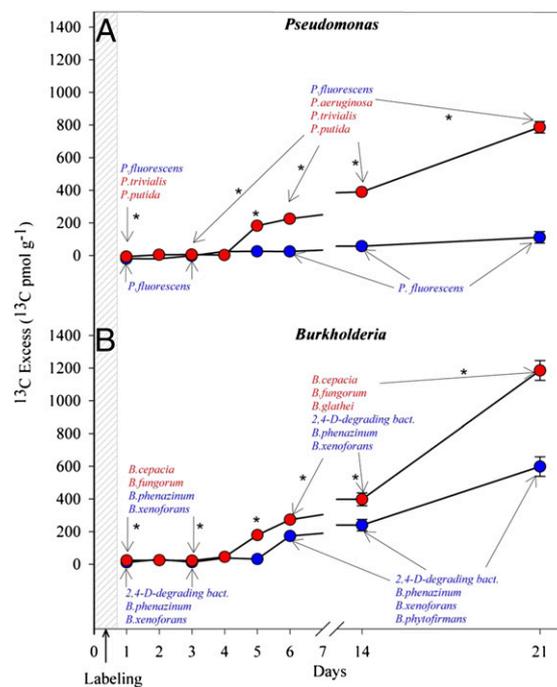
Fig. 3. ^{13}C enrichment in the rhizosphere of *F. rubra* at ambient (blue) and elevated CO_2 (red) in the PLFAs of (*A*) *Pseudomonas*- and (*B*) *Burkholderia*-specific signatures. For *C. arenaria*, *Pseudomonas* and *Burkholderia* showed the highest ^{13}C enrichment on day 1 at elevated CO_2 (Fig. S6). The active *Pseudomonas* and *Burkholderia* species identified by RNA-SIP, PCR-DGGE, and cloning are indicated along the time course at ambient and elevated CO_2. The species active only at elevated CO_2 are in red. Asterisks ($P < 0.001$) designate significant differences between CO_2 concentrations. The values given are the average of the different biological replicates, and errors represent the standard error. Points without error bars mean that the error falls within the size of the symbol designating the point.

kholderia (10). We observed that trehalose concentrations in the mycorhizosphere increased by 4-fold under elevated atmospheric CO_2 conditions [4.54 ppm (elevated CO_2) vs. 1.21 ppm (ambient CO_2)]. This suggests that AMF-associated trehalose release may be involved in inducing the observed shifts in active bacterial populations in the rhizosphere of *F. rubra*. As expected, no appreciable levels of trehalose were detected in the rhizosphere of the nonmycorrhizal plant, *C. arenaria*.

Bacillus spp. and actinomycetes have been recognized as typical bulk-soil inhabitants (20). Using the PLFA signatures i17:0 for *Bacillus* spp. (23) and 10Me-PLFAs for actinomycetes (24), we detected virtually no labeling for these groups throughout the experiment for both plant species studied (Fig. S3*B*). These results are consistent with previous findings that slow-growing soil microorganisms, such as actinomycetes, were unaffected by elevated CO_2 (25) and are supported by the fact that we detected no Actinobacteria- or Firmicutes-like sequences in our ^{13}C-based bacterial clone libraries.

In the controlled growth systems used in our experiment, we were able to follow carbon incorporation patterns to different components of the soil-borne microbial community, revealing major shifts in carbon-flow routes and active diversity after 6 months of exposure to elevated atmospheric CO_2 conditions. It should be noted that these effects may have been enhanced by the large and discrete shift in CO_2 conditions in our experiment, because it has been suggested that long-term gradual increases in CO_2 may have more subtle effects on plant–soil systems (26). Also, it is not yet clear how results obtained under controlled laboratory conditions will com-
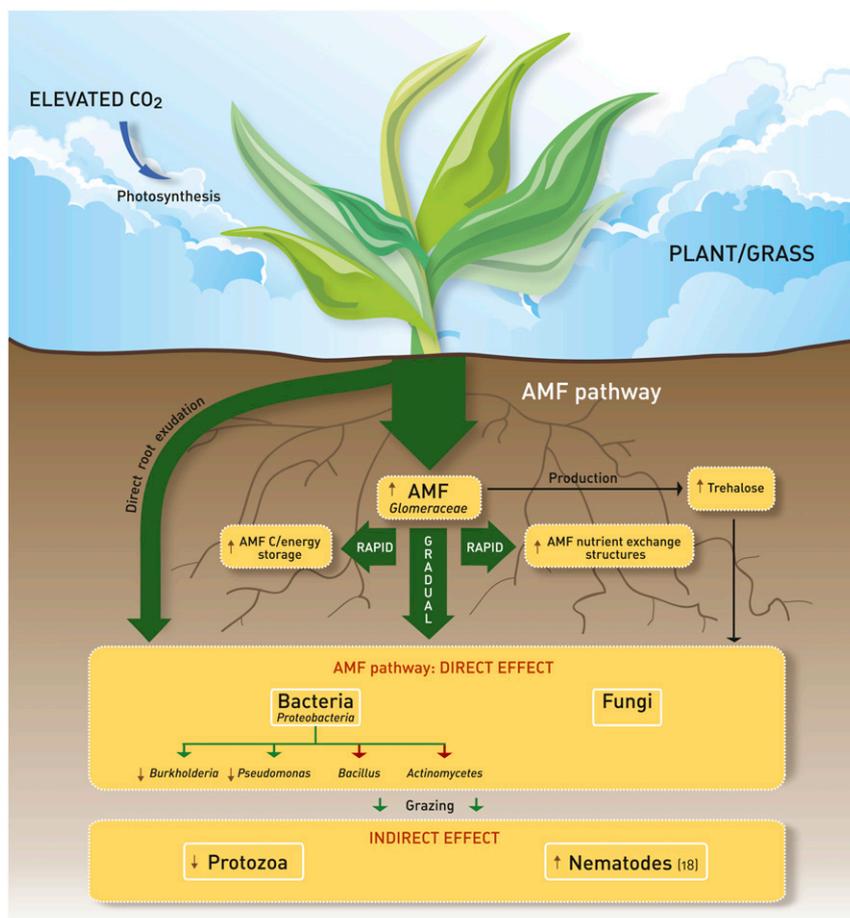
Fig. 4. Conceptual model of C flow in mycorrhizal plant–soil systems summarizing the observed effects of elevated CO_2 atmospheric concentrations on soil communities. Brown arrows indicate increases and decreases in the respective community sizes, as determined by real-time PCR and lipid analyses from this study and ref. 18, as well as changes in community structure and carbon flow. Absence of an arrow indicates no significant change in the community size or structure. Red arrows indicate no effect of increased C availability because of elevated CO_2 on the *Actinomycetes* spp. and *Bacillus* spp. communities. The mechanism and magnitude of the C flow along the soil–food web are indicated by the green arrows. Effects on nematodes are based on ref. 18.

pare with actual responses in the field, where environmental conditions are more variable.

Fig. 4 presents a conceptual model of C flow in mycorrhizal plant–soil systems and responses to elevated CO_2 conditions, summarizing our results. For mycorrhizal plants, allocation of labile photosynthates belowground proceeds principally through the AMF, which rapidly receive plant-derived C. AMF subsequently release this C gradually to their associated microbes, highlighting the keystone position of AMF in the release of plant-derived C to the soil microbial community. Shifts in AMF populations in response to elevated CO_2 conditions, therefore, result in marked changes in bacterial diversity and activity, stimulating the specific populations best capable of responding to the altered nutrient conditions of the (myco-)rhizosphere. Together, these responses may not only impact community structure and biodiversity of the microbial communities in the rhizosphere, but they may also affect carbon-turnover processes in soil and as such, the direction and magnitude of terrestrial ecosystem feedbacks in response to enhanced atmospheric CO_2 levels.

Materials and Methods

Plant and Soil Study Systems. Soil was collected from a river dune at Bergharen, The Netherlands (51°51′31.37″ N; 5°40′9.86″ E), where *F. rubra* and *C. arenaria* were the dominant grass and sedge species, respectively. The soil had a sandy texture, pH of 4.32, a low calcium carbonate content, and 1.97%

organic C, and it showed 1.7 mg/kg fungal biomass (estimated from ergosterol data). Ten soil cores (5–15 cm depth) were collected from 4 × 4-m sampling plots covered by *F. rubra* and *C. arenaria*. Pots were filled with sieved soil (1 kg), planted with three 4-wk-old seedlings of *F. rubra* and *C. arenaria*, and allocated to four CO_2 flow cabinets (a detailed description is in ref. 18). Two hundred pots per CO_2 (350 ppm and 700 ppm) and plant species (*F. rubra* and *C. arenaria*) treatment were grown for 6 months (211 total growing days) before the described pulse-chase ^{13}C-labeling experiment. *F. rubra* plants were found to be heavily colonized by AMF.

$^{13}CO_2$ Pulse Labeling. $^{13}CO_2$ pulse labeling (99% at ^{13}C–CO_2; Cambridge Isotope Laboratories) was carried out at 350 ppm or 700 ppm for the corresponding CO_2 treatments. A total of 150 *F. rubra* and 150 *C. arenaria* plants, plus 16 unplanted pots, were subjected to $^{13}CO_2$ pulse labeling, one-half from the 350-ppm CO_2 treatment and the other one-half from the 700-ppm CO_2 treatment. The remaining pots, used for natural abundance and background ^{13}C/^{12}C measurements, were incubated in two separate CO_2 flow cabinets (350 and 700 ppm) to ensure that there was no contamination with respired ^{13}C-enriched CO_2. The amount of $^{13}CO_2$ added during labeling was sufficient to label plants to 2,545‰ δ^{13}C at ambient CO_2 levels and 2,892‰ δ^{13}C at elevated CO_2. Actual ^{13}C content (excess ^{13}C) in individual pools (shoots, roots, and soil) was also calculated as described in ref. 27 (Fig. S4). Total RNA was extracted using the method described by refs. 13 and 14. RNA was chosen, as opposed to DNA, because of the more responsive accumulation of heavy isotope label in this nucleic acid pool (13). The integrity of the RNA preparations was visualized by LabChip microfluidic technology and automated electrophoresis for RNA analysis using the Experion RNA StdSens analysis system (Experion; Bio-Rad Laboratories). Total RNA was quantified

using both the Experion system and a NanoDrop ND-1000 Spectrophotometer (Bio-Rad Laboratories) and subsequently, was stored at −80 °C. ^{13}C-enriched RNA was obtained by density-gradient centrifugation and analyzed as described in ref. 15. RNA samples from equilibrium density gradient fractions were reverse transcribed using Moloney Murine Leukemia Virus reverse transcriptase with low RNase H activity (200 u/μl, ReverseAid M-MuLVRT; Fermentas) using random hexaminer primers (0.2 μg/μL), according to the manufacturer's protocol (RevertAid First Strand cDNA Synthesis Kit; Fermentas). The resulting cDNA was then used for bacterial 16S rRNA and fungal 18S rRNA quantification by real-time PCR using the Absolute Real-time PCR SYBR-Green mix (AbGene) on a Rotor-Gene 3000 (Corbett Research). All mixes were made using a CAS-1200 pipetting robot (Corbett Research). Quantification of fungal and bacterial small subunit ribosomal RNA cDNA copies in rhizosphere soil was carried as described in ref. 18 (Fig. S5). All of the samples and all standards were assessed in at least two different runs to confirm the reproducibility of the quantification. PCR-DGGE analysis of bacterial, fungal, *Pseudomonas* sp., *Burkholderia* ssp., and AMF communities of reverse-transcribed density-resolved RNA fractions followed the procedures described in refs. 18–31.

Cloning and Sequencing of Amplicons. PCR products derived from RNA templates and excised DGGE bands were obtained using several group-specific primer combinations as described in refs. 18, 27, 29, and 30. PCR products were purified with the High-Pure PCR Purification Kit (Boehringer Mannheim) and cloned into the pGEM-T Easy Vector (Promega), according to the manufacturer's instructions. Plasmid extraction was performed using the Wizard Plus SV Miniprep DNA Purification Kit (Promega); 1,350 clones, with confirmed inserts of the expected size, were selected randomly for sequencing using the vector-encoded universal T7 primer from the bacterial-, fungal-, *Pseudomonas*-, *Burkholderia*-, and AMF-specific libraries (Macrogen). Three different colonies with the expected insert were sequenced per excised band to confirm reliability of sequences derived from DGGE bands. Sequences were aligned in the Bioedit Sequence Alignment Editor program (www.mbio.ncsu.edu/BioEdit/bioedit.html). To identify chimeric sequences in the clone libraries, all recovered sequences were checked using CHIMER-A_CHECK 2.7 (Ribosomal Database Project II; http://rdp.cme.msu.edu). All

full-length and cloned bacterial (∼900 bp), *Pseudomonas* (∼250 bp), and *Burkholderia* (∼500 bp) 16S rRNA gene sequences and fungal (∼600 bp) and AMF (∼400 bp) 18S rRNA gene sequences were compared at the species level with sequences in public databases by using National Center for Biotechnology Information Blast (http://www.ncbi.nlm.nih.gov/blast) and the Ribosomal Database Project II Classifier (http://rdp.cme.msu.edu). To estimate the probability of observing differences in the frequency between libraries recovered from ambient and elevated CO_2 treatments, the cloned sequences were compared with the classification and library-compare algorithm published in naïve Bayesian Classifier for Rapid Assignment of rRNA Sequences (Ribosomal Database Project II).

Lipid Biomarker and Stable Isotope Analysis. NLFAs and PLFAs were extracted and analyzed according to the protocol described in ref. 27. The N/PLFA 16:1ω5 was used as a signature for AMF biomass and ^{13}C incorporation (12). The following fatty acids were used as biomarkers for bacterial biomass: i14:0, i15:0, a15:0, i16:0, 16:1ω7t, i17:1ω7, 10Me16:0, a17:1ω7, i17:0, a17:0, cy17:0, 10Me17:0, 18:1ω7c, 10Me18:0, and cy19:0 (24). PLFAs cy17:0 and cy19:0 were used as biomarkers for *Pseudomonas* spp. and *Burkholderia* spp., respectively (21). 10Me16:0, 10Me17:0, and 10Me18:0 were used for actinomycetes (24), and i17:0 was used for *Bacillus* (23). The signature 20:4ω6 was used to assess the ^{13}C incorporation and biomass of the protozoan community (19).

Neutral/phosphate lipid fatty acids were analyzed using ANOVA (Statistica 7.0; StatSoft) according to a split-plot design, considering the two different CO_2 treatments as a whole plot, with *F. rubra* and *C. arenaria* un/labeled, un/labeled unplanted soil, and the sampling times as subtreatments within each whole plot. The F statistic obtained by dividing the treatment mean square by the mean square for CO_2 flow cabinets was nested within CO_2 treatments.

1. Intergovernmental Panel on Climate Change (2007) Climate Change 2007 Synthesis Report. Summary for Policymakers. Available at www.ipcc.ch. Accessed November 1, 2007.
2. Ainsworth EA, Long SP (2005) What have we learned from 15 years of free-air CO_2 enrichment (FACE)? A meta-analytic review of the responses of photosynthesis, canopy properties and plant production to rising CO_2. *New Phytol* 165:351–371.
3. Strand AE, Pritchard SG, McCormack ML, Davis MA, Oren R (2008) Irreconcilable differences: Fine-root life spans and soil carbon persistence. *Science* 319:456–458.
4. Körner C, Arnone JA, 3rd (1992) Responses to elevated carbon dioxide in artificial tropical ecosystems. *Science* 257:1672–1675.
5. Zhou GY, et al. (2006) Old-growth forests can accumulate carbon in soils. *Science* 314:1417.
6. Pendall E, et al. (2004) Below-ground process responses to elevated CO_2 and temperature: A discussion of observations, measurement methods, and models. *New Phytol* 162:311–322.
7. Phillips RP (2007) Towards a rhizo-centric view of plant-microbial feedbacks under elevated atmospheric CO_2. *New Phytol* 173:664–667.
8. Carney KM, Hungate BA, Drake BG, Megonigal JP (2007) Altered soil microbial community at elevated CO_2 leads to loss of soil carbon. *Proc Natl Acad Sci USA* 104:4990–4995.
9. Fitter AH (2005) Darkness visible: Reflections on underground ecology. *J Ecol* 93:231–243.
10. Frey-Klett P, Garbaye J, Tarkka M (2007) The mycorrhiza helper bacteria revisited. *New Phytol* 176:22–36.
11. Staddon PL (2005) Mycorrhizal fungi and environmental change: The need for a mycocentric approach. *New Phytol* 167:635–637.
12. Olsson PA, Johnson NC (2005) Tracking carbon from the atmosphere to the rhizosphere. *Ecol Lett* 8:1264–1270.
13. Whiteley AS, Thomson B, Lueders T, Manefield M (2007) RNA stable-isotope probing. *Nat Protoc* 2:838–844.
14. Vandenkoornhuyse P, et al. (2007) Active root-inhabiting microbes identified by rapid incorporation of plant-derived carbon into RNA. *Proc Natl Acad Sci USA* 104:16970–16975.
15. Boschker HTS, et al. (1998) Direct linking of microbial populations to specific biogeochemical processes by ^{13}C-labelling of biomarkers. *Nature* 392:801–805.
16. Johnson D, Leake JR, Ostle N, Ineson P, Read DJ (2002) *In situ* ^{13}CO_2$ pulse-labeling of upland grassland demonstrates a rapid pathway of carbon flux from arbuscular mycorrhizal mycelia to the soil. *New Phytol* 153:327–334.
17. Maherali H, Klironomos JN (2007) Influence of phylogeny on fungal community assembly and ecosystem functioning. *Science* 316:1746–1748.
18. Drigo B, et al. (2007) Impact of elevated carbon dioxide on the rhizosphere communities of *Carex arenaria* and *Festuca rubra*. *Glob Change Biol* 13:2396–2410.
19. Mauclaire L, Pelz O, Thullner M, Abraham WR, Zeyer J (2003) Assimilation of toluene carbon along a bacteria-protist food chain determined by ^{13}C-enrichment of biomarker fatty acids. *J Microbiol Methods* 55:635–649.
20. Smalla K, et al. (2001) Bulk and rhizosphere soil bacterial communities studied by denaturing gradient gel electrophoresis: Plant-dependent enrichment and seasonal shifts revealed. *Appl Environ Microbiol* 67:4742–4751.
21. Vancanneyt M, Witt S, Abraham W-R, Kersters K, Fredrickson HL (1996) Fatty acid content in whole-cell hydrolysates and phospholipid fractions of pseudomonads: A taxonomic evaluation. *Syst Appl Microbiol* 19:528–540.
22. Gamper H, Hartwig UA, Leuchtmann A (2005) Mycorrhizas improve nitrogen nutrition of Trifolium repens after 8 yr of selection under elevated atmospheric CO2 partial pressure. *New Phytol* 167:531–542.
23. Kaneda T (1991) Iso- and anteiso-fatty acids in bacteria: Biosynthesis, function, and taxonomic significance. *Microbiol Mol Biol Rev* 55:288–302.
24. Frostegård A, Tunlid A, Bååth E (1993) Phospholipid fatty-acid composition, biomass and activity of microbial communities from 2 soil types experimentally exposed to different heavy-metals. *Appl Environ Microbiol* 59:3605–3617.
25. Bardgett RD, et al. (1999) Below-ground microbial community development in a high temperature world. *Oikos* 85:193–203.
26. Klironomos JN, et al. (2005) Abrupt rise in atmospheric CO_2 overestimates community response in a model plant-soil system. *Nature* 433:621–624.
27. Boschker H (2004) Linking microbial community structure and functioning: stable isotope (^{13}C) in combination with PLFA analysis. *Molecular Microbial Ecology Manual II*, eds Kowalchuk GA, et al. (Kluwer, Dordrecht, The Netherlands), pp 1673–1688.
28. Treonis AM, et al. (2004) Identification of groups of metabolically-active rhizosphere microorganisms by stable isotope probing of PLFAs. *Soil Biol Biochem* 36:533–537.
29. Garbeva P, Veen JA, Elsas JD (2004) Assessment of the diversity, and antagonism towards Rhizoctonia solani AG3, of *Pseudomonas* species in soil from different agricultural regimes. *FEMS Microbiol Ecol* 47:51–64.
30. Salles JF, De Souza FA, van Elsas JD (2002) Molecular method to assess the diversity of *Burkholderia* species in environmental samples. *Appl Environ Microbiol* 68:1595–1603.
31. Gollotte A, Van Tuinen D, Atkinson D (2004) Diversity of arbuscular mycorrhizal fungi colonising roots of the grass species *Agrostis capillaris* and *Lolium perenne* in a field experiment. *Mycorrhiza* 14:111–117.